

COVENTRY UNIVERSITY

FINAL YEAR PROJECT

AUTHOR: Stefan Hristov Asenov

SUPERVISOR: Dr. Stratis Kanarachos

**FACULTY OF ENGINEERING, ENVIRONMENT AND
COMPUTING DEPARTMENT OF MECHANICAL,
AEROSPACE AND AUTOMOTIVE ENGINEERING**

**TITLE: *Measurement and Analysis of strains developed
on tie-rods of a steering system***

**SUBMITTED IN PARTIAL FULFILMENT OF THE
REQUIREMENTS FOR THE DEGREE OF BACHELOR OF
ENGINEERING**

YEAR 2016

SUBMISSION DATE 25/04/16

DECLARATION

The work described in this report is the result of my own investigations. All sections of the text and results that have been obtained from other work are fully referenced. I understand that cheating and plagiarism constitute a breach of University Regulations and will be dealt with accordingly.

Signed: *Stefan Asenou*

Date: 25/04/16

Abstract

Modern day manufacturers research and develop vehicles that are equipped with steering assist to help drivers undertake manoeuvres. However the lack of research for a situation where one tie-rod experiences different strains than the opposite one leads to failure in the tie-rod assembly and misalignment in the wheels over time. The performance of the steering system would be improved if this information existed. This bachelor's dissertation looks into this specific situation and conducts an examination on the tie-rods.

A simple kinematic model is used to determine how the steering system moves when there is a steering input. An investigation has been conducted to determine how the system's geometry affects the strains.

The experiment vehicle is a Formula Student car which is designed by the students of Coventry University. The tests performed show the difference in situations where the two front tyres are on a single surface, two different surfaces – one with high friction, the other with low friction and a situation where there's an obstacle in the way of one of the tyres.

The experiment results show a major difference in strain in the front tie-rods in the different situations. Interesting conclusions can be made due to the results for the different surface situation where one of the tyres receives similar results in both compression and tension, but the other one receives results with great difference.

This results given in the report can be a starting ground and help with the improvement in steering systems if more research is conducted.

Acknowledgements

This bachelor's degree dissertation was completed at the Faculty of Engineering, Environment and Computing at Coventry University. Firstly I want to

express my deepest gratitude to Coventry University for giving me the opportunity to study in this organisation.

Special appreciation to Dr. Stratis Kanarachos for being my supervisor, providing a topic to conduct a study on when I was left without one and also helping me throughout my dissertation.

A special thanks to Mr. James Jarvis, Dr. Gary Wood, Mr. Georgios Chrysakis and Mr. Bill Dunn for helping me to develop an understanding for solid mechanics, vehicle systems and vehicle dynamics and also making the subjects interesting and engaging.

I would also like to take this opportunity to give credit to Mr. Ricky Atwal for providing the needed help to secure a placement position which later helped me to secure a graduate role as well.

Last but not least I would like to give my deepest gratitude to Mr. Ashley Lees, Mr. Steve Poote and Mr. Paul Green for being my tutors during my years in the University and helping me develop myself as a professional. From day one those people have been showing me how the industry is working and they have given me guidance on how to establish myself as an Engineer.

Table of contents

DECLARATION	2
Abstract.....	3
Acknowledgements.....	3
Table of contents	5
Abbreviations.....	7
List of Figures, Graphs, Pictures and Tables	8
1. Introduction	10
2. Literature Review.....	11
2.1. Power Steering.....	11
2.1.1. Hydraulic pump.....	11
2.1.2. Fluid reservoir	12
2.1.3. Fluid Lines.....	12
2.1.4. Rotary valve.....	12
2.1.5. Piston-cylinder assembly	12
2.2. Forces on the steering system	13
2.2.1. Forces and moments in tyre.	13
2.2.2. Tyre force and moments transformation in to axial force in tie-rods	15
2.3. Ways to analyse mechanisms and frictions	16
3. Preparation for the experiment.....	17
3.1. Representation of kinematic model	17
3.2. Cornering stiffness study	19
3.3. Design and preparation for test.....	20
3.3.1. Strain measuring	20
3.3.2. Methodology for experiment.....	21
3.3.3. Calculations and research for tie-rods.....	22
4. Test and analysis.....	23
4.1. First test readings, calculations and results.....	23
4.2. Second Test Readings and Results	25
4.3. Comparison between first and second test	27
4.4. Third Test Readings, Results and Discussion	28

5. Conclusions	31
6. Proposal for future applications.	31
Bibliography	32
References	32
Appendix	34

Abbreviations

kg – Kilogram

m – Meter

mm – Milimeter

Pa – Pascal

N – Newton

N/m² – N

Ø – Diameter

° - Degree

R – Radius

F_{TRL} – Force on left tie-rod

F_{TRR} – Force on right tie-rod

F_D – Transferred Force from pinion

M_D – Pinion Moment

F_M – Power steering Force

M_z – Aligning moment

F_y – Lateral Force

μ - Friction Coefficient

F_{y0}($\frac{\mu}{\mu_0} \alpha_f$) - Template function of the lateral force characteristic

SAT – Self Aligning Torque

T_{sat} – Torque of Self-aligning torque

T_{sat0}($\frac{\mu_0}{\mu} \alpha_f$) - Template function of the SAT characteristic

M_{kp} – Kingpin Moment

t_{CAS} – Caster Trail

F_{YF} – Tyre lateral Force

F_T – Tie-rod Force

L_K – Knuckle arm Length

μ₀ – Friction Coefficient or Link Efficiency

C_α – Cornering Stiffness

F_z – Forces acting on front and rear axles

R1, R2, R3, R4 – Resistors

E – Voltage source or Young's Modulus

e₀ – Multimeter

N/rad – Newtons per radian

m/s – Meters per second

R_G – Strain gauge with Resistance

Π – Pi=3.14

A – Area

V – Volt

g – Earth's acceleration

σ – Stress

L – Length

ε - Strain

List of Figures, Graphs, Pictures and Tables

Figure (1) Power steering system

Figure (2) Hydraulic pump and reservoir

Figure (3) Piston-cylinder assembly, rotary valve and fluid lines.

Figure (4) Mr. Matilainen simplified model.

Figure (5) Characteristics of tyre lateral force and SAT

Figure (6) Transformation of tyre torque and lateral force to tie-rod force

Figure (7) Wheatstone bridge

Figure (8) Wheatstone bridge with three wire setting

Graph (1) Change in length of left hand tie-rod in first two tests

Graph (2) Change in length of right hand tie-rod in first two tests

Graph (3) Change in length in third test

Picture (1) Formula student car – Aligned tyres

Picture (2) Formula student car – Right steering input

Table (1) Vehicle dimensions

Table (2) Weight equivalence to Resistance

Table (3) First test readings

Table (4) Force in first test

Table (5) Stress in first test

Table (6) Strain in first test

Table (7) Displacement in first test

Table (8) Second test readings

Table (9) Force in second test

Table (10) Stress in second test

Table (11) Strain in second test

Table (12) Displacement in second test

Table (13) Third test readings

Table (14) Force in third test

Table (15) Stress in third test

Table (16) Strain in third test

Table (17) Displacement in third test

1. Introduction

Front wheel alignment in vehicles is important for the conservation of tyres and prevention of tie-rod assembly failure. This report will cover an investigation of a vehicle in a static state that performs a parking manoeuvre in a normal day environment. The purpose is to find the strains developed during those manoeuvres and possibly provide a solution to help with the issues stated above.

The report will be separated in sections to describe the approach of solving the stated issues. It will give information about previous research in the area and will provide evidence of tests conducted that measure developed strains in different scenarios.

The analysis of the tests will give an explanation how and why those strains are developed and what differences are occurring during the different manoeuvres. It will also give a proposal for future applications that will help with the solution of the raised issues.

The aims of the project are to develop an understanding of the behaviour of the steering system and to develop an understanding on how strains on the tie-rods are developed under different conditions.

The objectives of the project are to conduct a research and review on literature for the steering systems and to create a simple kinematic model of the steering system. Another set of objectives is to design and conduct measurement tests of the strains under different conditions. Following the analysis of the results, a conclusion will be made and a proposal for future applications.

2. Literature Review

2.1. Power Steering

The power steering is used to ease the work of a driver during cornering. The system consists of a fluid reservoir, a pump, rotary valve, fluid lines and a piston-cylinder assembly.

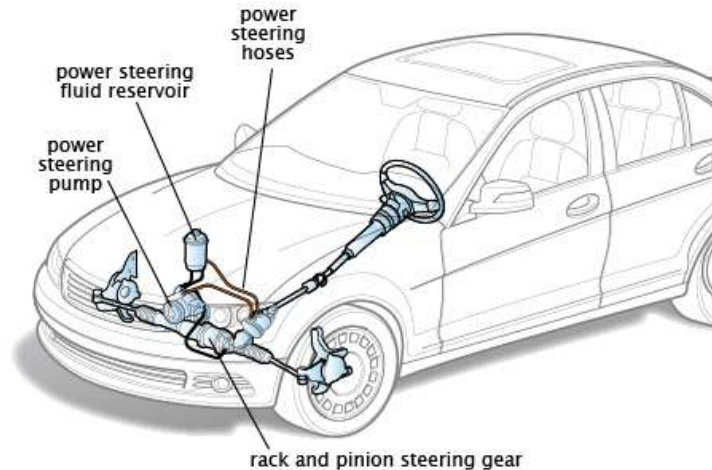


Figure (1) Power steering system (Repairpal, 2016)

2.1.1. Hydraulic pump

The hydraulic pump is connected and receives its power from the engine via a pulley and a belt. The inside of the pump consists of a rotary assembly that has retractable vanes which control the amount of fluid that goes to the rotary valve, i.e. when there's a steering input from the driver, the assembly forces more fluid through the lines. The hydraulic pump also has a relief valve that controls the amount of pressure in the system.

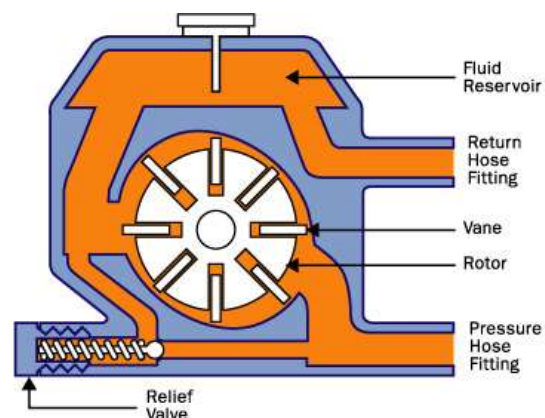


Figure (2) Hydraulic pump and reservoir (Enginebasics, 2010)

2.1.2. Fluid reservoir

The fluid reservoir contains the fluid of the system. It has an inlet and an outlet which transfers the fluid to and from the hydraulic pump. When the pressure after the hydraulic pump raises too high, the relief valve returns opens to return part of the fluid back to the reservoir to prevent failure due to high pressure.

2.1.3. Fluid Lines

The fluid lines transfer the fluid along the system. They can be either low pressure return hoses or high pressure hoses that transfer the fluid from the hydraulic pump to the rotary valve and from the rotary valve to the piston-cylinder assembly.

2.1.4. Rotary valve

As seen on figure (3), the rotary valve controls the amount of fluid which is sent to each of the sides of the piston-cylinder assembly. The torsion bar which is connected to the steering wheel and the pinion is also connected to the inner valve of the rotary valve assembly. Depending on the direction where the driver introduces steering input, the rotary valve advances more fluid into the chosen fluid line and thus provides assistance for the driver.

2.1.5. Piston-cylinder assembly

Figure (3) Shows the piston-cylinder assembly and how it is a part of the steering rack. As stated above, the fluid is transferred to the pistons via the fluid lines. Depending on the direction of turning, the hydraulic fluid is added to one side of the cylinder and withdrawn from the other side. This results in an assistance on the pinion.

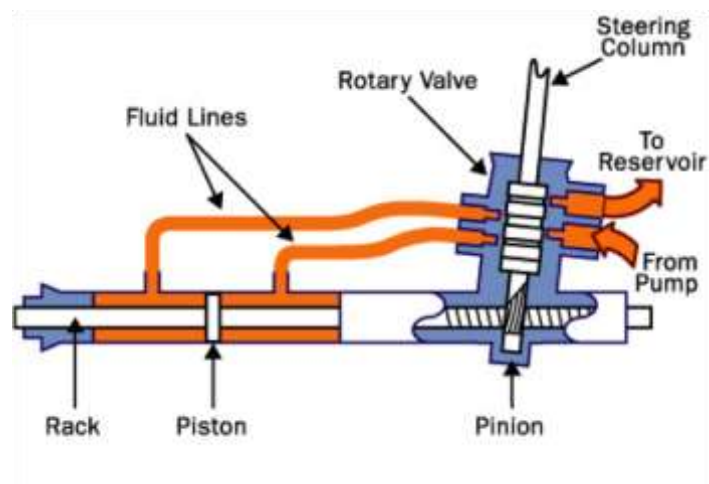


Figure (3) Piston-cylinder assembly, rotary valve and fluid lines. (Howstuffworks, 2016)

2.2. Forces on the steering system

To examine the forces and strains on the tie-rods a simplified model needs to be created. Mika J. Matilainen provides a model in his conference paper on Tyre friction potential estimation from measured tie rod forces.

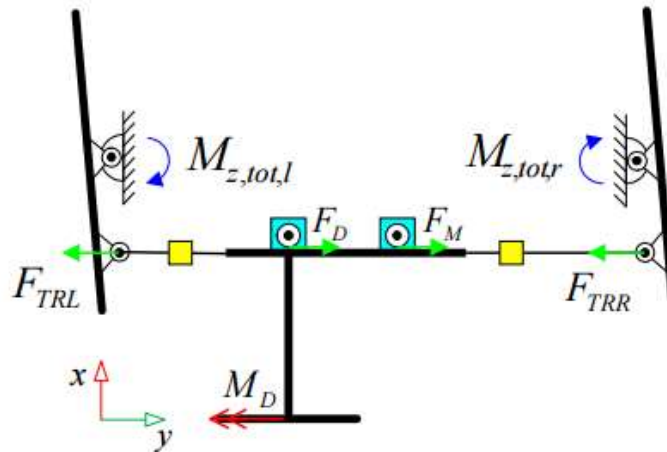


Figure (4) Mr. Matilainen simplified model. (Matilainen, 2011)

After an investigation on this model, it can be said that the forces acting on the left and right tie rods (F_{TRL} and F_{TRR}) are the equivalent to the combined force generated from the transferred steering input moment M_D to force F_D and the force from the power steering input F_M :

$$F_{TRL} + F_{TRR} = F_D + F_M$$

The aligning torques M_z in each wheel are generated from the lateral tyre forces around the steering axes (Matilainen, 2011). The yellow boxes in the figure represent the strain gauges fitted on the tie rods and depending on the direction of steering one will be in compression, the other in tension.

The two steering input forces aren't the only factors that create tension and compression in the tie-rods. The friction between the tyres and the surface create forces and moments that are transferred to the tie-rods through the kingpin. Following is an explanation on how those forces and moments are generated and transmitted:

2.2.1. Forces and moments in tyre.

Takuro Matsuda says that the sensitivity of lateral force to the friction coefficient is modelled by the similarity transformation method (Matsuda et al, 2013) and it can be expressed in the following formula:

$$F_y = \frac{\mu}{\mu_0} F_{y0} \left(\frac{\mu}{\mu_0} \alpha_f \right)$$

Where F_y denotes the lateral force and μ is the friction coefficient. $F_{y0} \left(\frac{\mu}{\mu_0} \alpha_f \right)$ is a template function of the lateral force characteristic measured experimentally on a road surface having and its friction coefficient μ_0 .

The Self-aligning torque formula has a similar method of expression

$$T_{\text{sat}} = \frac{\mu_0}{\mu} F_{\text{sat}0} \left(\frac{\mu_0}{\mu} \alpha_f \right)$$

Where T_{sat} denotes SAT, and $T_{\text{sat}0} \left(\frac{\mu_0}{\mu} \alpha_f \right)$ is a template function of the SAT characteristic measured experimentally on a road surface and its friction coefficient μ_0 .

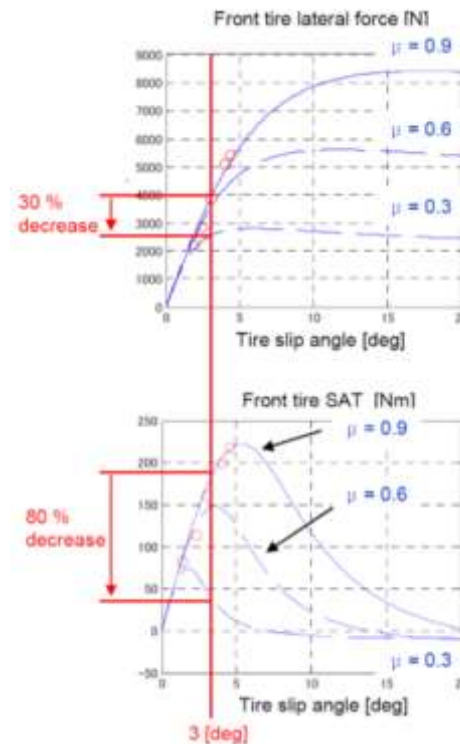


Figure (5) Characteristics of tyre lateral force and SAT (Matsuda et al., 2013)

In the report *Instantaneous Estimation of Road Friction based on Front Tire SAT using Kalman Filter*, Takuro Matsuda et al show a comparison between friction coefficients of the self-aligning torque and front tire lateral force. The comparison is looked at a 3° tire slip angle. While the friction coefficient drop in the tire lateral force has a 30% decrease in force, the SAT receives an 80% decrease in moment, which suggests that the SAT is much more sensitive to regarding friction coefficient and

utilizing SAT information extensively improves μ estimation performance in low lateral acceleration cornering maneuvers in comparison with conventional methods that only refer to lateral force. (Matsuda et al., 2013)

2.2.2. Tyre force and moments transformation in to axial force in tie-rods

Tyre force and torque generated from steering are transferred to the tie rods. Figure (6) shows how the kingpin torque consists of Self Aligning Torque (SAT) and Tyre lateral force. Following those statements a mathematical model can be written as

$$M_{kp} = T_{SAT} + t_{CAS} * F_{YF}$$

Where M_{kp} is the moment in the kingpin, T_{SAT} is the Self aligning torque, F_{LF} is the tyre lateral force and the t_{CAS} is the caster trail. As Matsuda says in his report that the components are per-axle and are obtained by as the sum of the forces acting on each tyre. He also says that contribution of jacking torque can be ignored because it is mutually cancelled due to the opposition of the tyres. (Matsuda, et al., 2013). The Kingpin torque is transformed to the tie-rod force via the knuckle arm, and thus the knuckle arm length needs to be considered with the link efficiency at 0 degree steering input. The equation can be generated as

$$F_T = \frac{M_{kp}}{\mu_0 * L_k}$$

Where F_T is the Tie-rod force, M_{KP} is known, the link efficiency is μ_0 and the knuckle arm length is L_K .

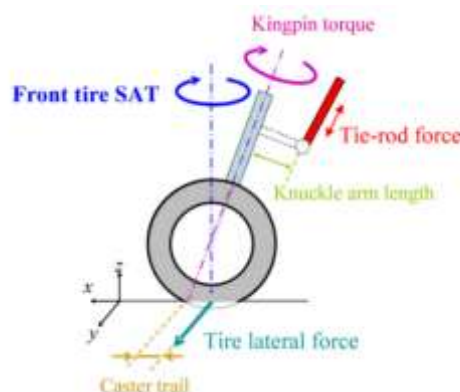


Figure (6) Transformation of tyre torque and lateral force to tie-rod force
(Matsuda et al., 2013)

2.3. Ways to analyse mechanisms and frictions

In order to receive an understanding on how the mechanisms receive loads and forces a research on methods need to be done. Three methods have been established to help with solving kinetoelastodynamic problems – The floating frame of reference method, the co-rotational formulation method and the finite segment method.

The floating frame of reference method has two sets of coordinates to describe the position of a flexible body, in which one describes the location and orientation and the other describes the deformation of the inspected body. This method is widely used because it suits with widely used computer software for FEA. (Kanarachos, 2008)

The co-rotational formulation method – where nodal coordinates, velocities, accelerations, incremental displacements and rotations, and equations of motion are defined in terms of the fixed global coordinates, while the strains in the element are measured in a set of element coordinates which is related with each element. (Kanarachos, 2008)

The finite segment is a method where the deformable body is assumed to consist of a set of rigid bodies which are connected by springs and/or dampers. Each rigid segment is defined using three independent Cartesian coordinates and four independent Euler parameters. This method is used because the complexity of the details of the system can be encapsulated into library blocks facilitating reuse and modification. (Kanarachos, 2008)

Due to the fact that the linear theory of beams needs to be able to perform large displacements in their analysis, in a journal named “*An incremental finite element analysis of mechanisms and robots*” Dr. Kanarachos and K. Spentzas say that an alternative method can be introduced to decompose large displacements in a series of successive small displacements. It is called the incremental method and is not a complicated approach due to the fact that at the end of any small displacement, the position of a deformed member of the mechanism gives the initial conditions for the displacement. The method requires only an adaptation of the software currently used for the finite element dynamic analysis of rectilinear elastic beams. (K. Spentzas, S. Kanarachos, 2002)

3. Preparation for the experiment.

Before the experiment can be conducted, the student has to measure the geometry of the vehicle and to design the tests that will simulate the parking manoeuver:

3.1. Representation of kinematic model

The tested vehicle will be the Formula Student car in the Coventry University workshop. Figure () shows the general dimensions of the car.

Dimension	Value
Front Tyres	Avon 7.2/20-R13 230mm
Tie-rod length	300mm
Wheelbase	1652mm
Total Mass	247 kg
Mass distribution : Front/Rear	48:52
Camber angle	2.5°
Centre of mass height	270mm
Outer tie-rod diameter	Ø16mm
Inner tie-rod diameter	Ø12mm

Table (1) Vehicle dimensions

Used equipment:

- Tape measure
- Micrometre
- Digital Vernier calliper

The information for the weight, Mass distribution and Camber angle was taken from the CAD file provided from Mr. James Jarvis at Coventry University. The following information represents the behaviour of the vehicle while having a right steering input.



Picture (1) Formula student car – Aligned tyres

As seen on the picture above the vehicle is lifted for easier measurements.

The first taken measurement is the distance between the tyres. Due to the fact that most racing cars have camber angles and so does the Formula Student car there's a slight difference between the top and bottom measurements:

- Top distance between tyres (centre to centre) – 1410 mm
- Bottom distance between tyres (centre to centre) – 1450 mm

The distance from the body to each tyre is as follows:

- On the right – 300 mm
- On the left – 300 mm



Picture (2) Formula student car – Right steering input

After introducing a steering input –dead right the following results are present:

- On the right (after steering input)– 430 mm
- On the left (after steering input)– 170 mm

Due to the wrong setting on the tie-rods, the rack distance on each side from the body is different when the tyres are aligned:

- On the right – 45 mm
- On the left – 67 mm

After the steering input is introduced it is observed that the rack travel is 30 mm:

- On the right (after steering input)– 75 mm
- On the left (after steering input)– 37 mm

3.2. Cornering stiffness study

A cornering stiffness study on the tyres can be beneficial for future applications and research using different models such as Brush Tyre model and the Bicycle mode.

$$C_{\alpha} = a_3 \left(\sin \left(2 \cdot \tan^{-1} \left(\frac{F_z}{a_4} \right) \right) \right)$$

Where a_3 is evaluated from $a_3 = -1236.2 \cdot x + 148744$ and a_4 is evaluated from $a_4 = 73.039 \cdot x - 5641.9$ which is a given formula from a lecture part of module 332MAE at Coventry University. x is the size of the tyre and F_z is the force acting on the front and rear axles.

$$F_{ZF} = \text{Total mass} \cdot \text{Front mass distribution} \cdot g = 247 \cdot 0.48 \cdot 9.81 = 1163.07 \text{ N}$$

$$F_{ZR} = \text{Total mass} \cdot \text{Rear mass distribution} \cdot g = 247 \cdot 0.52 \cdot 9.81 = 1260 \text{ N}$$

Using the tyre size of 230mm into the formulas for a_3 and a_4 the values received are -135582 and 11157.07 respectively. Substituting the forces and the values for a_3 and a_4 , the calculated cornering stiffness for the front tyres is -27964.345 N/rad and for the rear tyres is -30237.684 N/rad.

There is a simplified Bicycle model in the Appendix that uses the tyre cornering stiffness values and represents the situation where the Formula Student car is undertaking a manoeuvre with a low velocity of 2 m/s. The model can be adjusted for the designer's needs, but since this report is representing the situation where the car is static, the velocity of the Bicycle model is close to 0. The plotted results from the model represent the behaviour of the vehicle – The lateral forces it experiences, the body slip angle, the slip angle of the tyres, the angular displacement and velocity and the trajectory of the vehicle.

3.3. Design and preparation for test

The experiment will be performed in the High Performance Engineering Centre of the Coventry University's Engineering and computing building. The data will be gathered from piezo-electric strain gauge through Multimeter readings. Three different scenarios for parking manoeuvres will be looked into to gather data.

3.3.1. Strain measuring

The piezo-electric strain gauge is connected to a Wheatstone bridge system to receive the strains developed in the tie-rods. The Wheatstone bridge is used because it has the ability to detect small resistance changes (Vishay 2005).

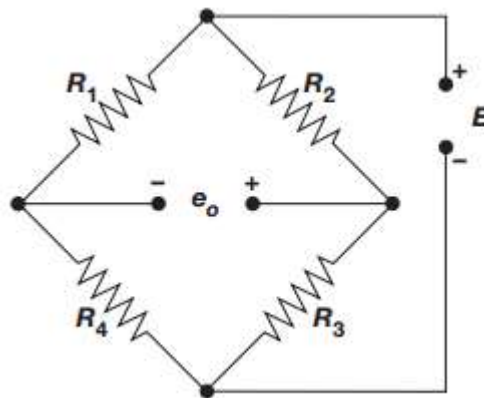


Figure (7) Wheatstone bridge (Intertechnology, 2016)

Figure (7) Represents the schematic of the Wheatstone bridge. It is made out of four Resistors – R_1 , R_2 , R_3 and R_4 , a voltage source – E and a multimeter e_0 . When

$$R_4/R_1=R_3/R_2$$

The system is balanced and the readings on the multimeter should show 0V. Using a strain gauge of the same resistance to replace one of the Resistors, the balance of the bridge will maintain 0 value. When the strain gauge is subjected to load, the bridge will be unbalanced and the readings will be taken from the multimeter. To connect the strain gauge to the bridge, one should use the following three wire diagram (Figure 8)

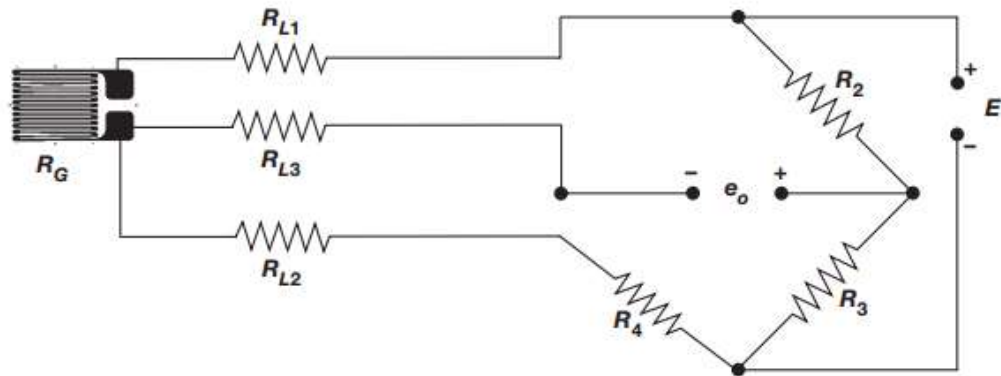


Figure (8) Wheatstone bridge with three wire setting (Intertechnology, 2016)

Where R_G is the Strain gauge. There is a diagram where the connection can be implemented using only two wire configuration but Vishay says that this will cause a resistance imbalance and thus the three wire configuration is used for more accurate readings (Vishay, 2005).

3.3.2. Methodology for experiment.

The experiment will cover three situations:

- the car doesn't have an obstacle and both of its tyres are on the same surface;
- the car has an obstacle next to the right tyre
- the two tyres are on different surfaces

In the first situation the car will be placed on the High Performance Engineering Centre's surface which is considered to have low friction coefficient. The two strain gauges will be fitted on each tie-rod and the readings will be transmitted to an amplifier via wiring conductor. From the amplifier each wire will be connected to a multimeter, one of which will have its readings dropping, and the other's reading raising. The student and Mr. James Jarvis will read the multimeter data and will be looking for peak values while there's an input onto the steering system. The experiment will consist of 6 tries that will give enough data to solidify the results. The steering input will be steady right direction.

The second experiment will be undertaken with an obstacle in the way of the front right tyre. Same as the previous experiment, there will be six tries that will show the difference between the first and the second tests. The readings will be then analysed and compared, and put onto an excel spreadsheet. The idea behind this test setting is to simulate parking manoeuvre where the vehicle is next to a road kerb and the tyre

and tie-rod on one side experience more resistance compared to the other side. The steering input will be the same as the previous setting – steady right direction.

For the last experiment, the Formula Student car will be placed on two different surfaces at the same time. The left hand tyre will be placed on a high-friction surface (Asphalt) and the right hand tyre will be placed on the same surface as previously. This setting is going to simulate a situation where the vehicle is undertaking a manoeuvre with one tyre on the asphalt and the other on a slippery surface such as ice, water or oil spillage. The research is performed to create an understanding whether a difference in surface friction coefficient will result in difference in strain. In this setting of the experiment, the steering input will be steady for both left and right directions to indicate any differences created by the changing car geometry.

Before the experiment can be conducted, a calibration on the strain gauges needs to be performed to indicate what values of volt represent the forces acting on the tie-rods. A set of weights is used to indicate different set loads.

Weight (kg)	Left Strain Gauge (V)	Right Strain Gauge (V)
0	2.03	1.03
1	2.04	1.02
6	2.09	0.97
11	2.14	0.92

Table (2) Weight equivalence to Resistance

Table (2) shows the resistance readings that are equivalent to the different loadings. It can be concluded that for each kilogram load, the equivalent resistance is 0.01V. Looking at the resistance values it can be seen that the Left Strain Gauge receives a raise in its values, whereas the Right Strain Gauge receives drop. This is caused by the fact that the readings are dimensionless and the direction of the change should be neglected.

3.3.3. Calculations and research for tie-rods

As stated in Table (1) the tie rods' outer and inner diameters are \varnothing 16mm and \varnothing 12mm respectively. To calculate their area the formula

$$A = \pi * (R_1^2 - R_2^2)$$

Is used, where A is the area, Π is pi and R_1 and R_2 are the outer and inner diameter, respectively. The material used to manufacture the tie-rods is Steel with a Young's Modulus of $E=210$ GPa. This data was taken from the CES2015 EduPack software (CES, 2015)

4. Test and analysis.

Dr. Kanarachos suggested that the first two experiments should be conducted first in order to gather data and decide, whether the differences between the experiments will generate difference in values that can be compared. The first two experiments took place on the 21st of March, 2016 and following a discussion with Dr. Kanarachos, the third experiment was decided to be performed as well – on the 19th of April, 2016. The report will give only examples of the conversions and tables will be inserted in the appendix.

4.1. First test readings, calculations and results

The first test was undertaken to set a benchmark for the results.

First Test		
Try	Left hand rod results (V)	Right hand rod results (V)
1	0.46	0.41
2	0.35	0.44
3	0.47	0.46
4	0.42	0.4
5	0.39	0.4
6	0.41	0.37
Avg.	0.42	0.41

Table (3) First test readings

Table (3) shows the raw results from the experiment. Following those results, a few calculations need to be performed to convert the results to strain and displacement.

To change the Resistance reading to load in kg the calibration equivalence needs to be inserted

$$0.01V=1kg$$

Following this equivalence, the result for the first try can be converted as

$$0.46V=46kg$$

The load in kg is then converted to Force in which

$$F=m*g$$

Where F is the force, m is the mass in kg and g is the acceleration in m/s

$$F=46*9.81=451.26N$$

The next step is to calculate the stress σ in the tie-rods.

$$\sigma=F/A$$

The formula above can be used to calculate the stress when the force and the area are known. In this try stress value is 1283.155 kPa. Continuing with the calculations, the next variable that can be calculated is the strain. As stated previously, the Young's Modulus is $E=210$ GPa. Using the formula

$$\epsilon= \sigma/E$$

and substituting the values, the result is $\epsilon= 0.006110263$. To calculate the change in length, the student used the following formula

$$L= (\sigma*L_0)/E$$

Where L is the change in length and L_0 is the initial length. For this experiment the calculated value is 0.0018m.

Using an excel spreadsheet one can easily calculate the remaining values for the three experiments. The results are given in the tables below.

	For left hand (N)	For right hand (N)
1	451.26	402.21
2	343.35	431.64
3	461.07	451.26
4	412.02	392.4
5	382.59	392.4
6	402.21	362.97

Table (4) Force in first test

	Stress For left hand (Pa)	Stress For right hand (Pa)
1	1283155.141	1143681.756
2	976313.6943	1227365.787
3	1311049.818	1283155.141
4	1171576.433	1115787.079
5	1087892.402	1115787.079
6	1143681.756	1032103.048

Table (5) Stress in first test

	Strain For left hand	Strain For right hand
1	0.006110263	0.005446104
2	0.004649113	0.005844599
3	0.006243094	0.006110263
4	0.005578935	0.005313272
5	0.00518044	0.005313272
6	0.005446104	0.004914776
AVG	0.005534658	0.005490381

Table (6) Strain in first test

	Displacement For left hand (m)	Displacement For right hand (m)
1	0.0018	0.0016
2	0.0014	0.0018
3	0.0019	0.0018
4	0.0017	0.0016
5	0.0016	0.0016
6	0.0016	0.0015
AVG	0.0017	0.0016

Table (7) Displacement in first test

Now that the benchmark is set, one can continue with the other experiments.

4.2. Second Test Readings and Results

Second Test		
Try	Left hand rod results (V)	Right hand rod results (V)
1	0.35	1.04
2	0.38	1.12
3	0.46	1.25
4	0.41	1.11
5	0.39	1.23
6	0.43	1.09
Avg.	0.40	1.14

Table (8) Second test readings

Observing Table (8), one can evaluate that the obstacle does affect the readings and the magnitude of the strains developed in the tie-rods are picked by the sensors. Using the same approach as with the first test, tables with the results can be produced.

	Force For left hand (N)	Force For right hand (N)
1	343.35	1020.24
2	372.78	1098.72
3	451.26	1226.25
4	402.21	1088.91
5	382.59	1206.63
6	421.83	1069.29

Table (9) Force in second test

	Stress For left hand (Pa)	Stress For right hand (Pa)
1	976313.6943	2901046.406
2	1059997.725	3124203.822
3	1283155.141	3486834.622
4	1143681.756	3096309.145
5	1087892.402	3431045.268
6	1199471.11	3040519.791

Table (10) Stress in second test

	Strain For left hand	Strain For right hand
1	0.004649113	0.013814507
2	0.005047608	0.014877161
3	0.006110263	0.016603974
4	0.005446104	0.014744329
5	0.00518044	0.016338311
6	0.005711767	0.014478666
AVG	0.005357549	0.015142825

Table (11) Strain in second test

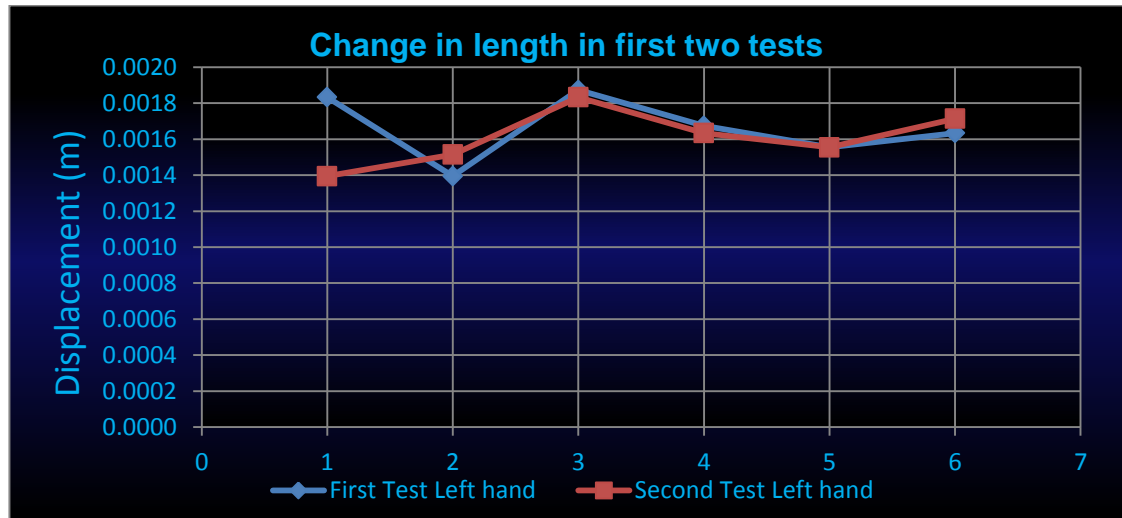
	Displacement For left hand (m)	Displacement For right hand (m)
1	0.0014	0.0041
2	0.0015	0.0045
3	0.0018	0.0050
4	0.0016	0.0044
5	0.0016	0.0049
6	0.0017	0.0043
AVG	0.0016	0.0045

Table (12) Displacement in second test

A further discussion will be done in the next section.

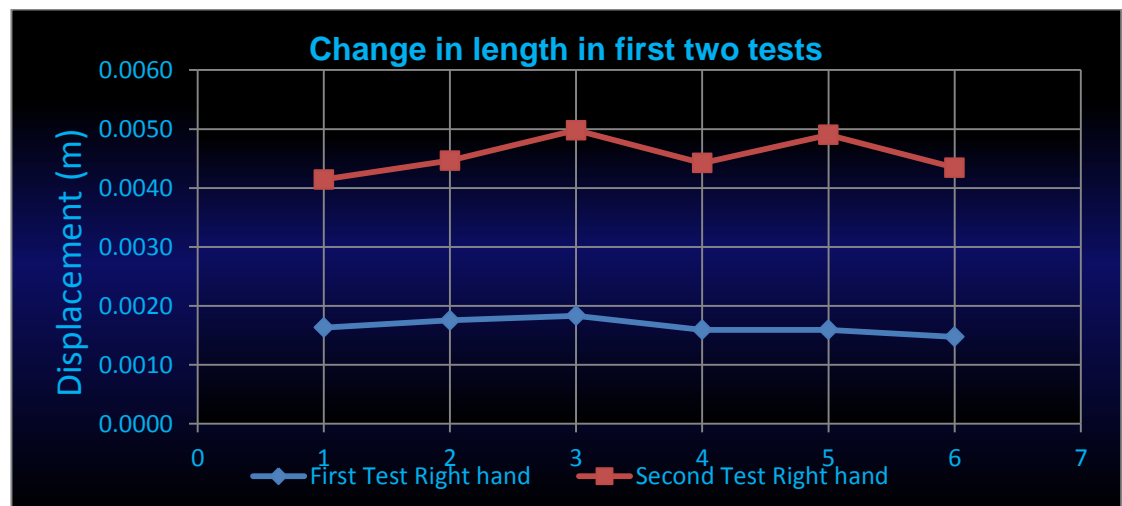
4.3. Comparison between first and second test

Comparison graphs can be produced using the data from the first and the second test.



Graph (1) Change in length of left hand tie-rod in first two tests

Graph (1) shows the calculated displacement experienced by the left hand tie-rod in the two experiments. Overall the displacement of the tie-rod is similar between the two tests, but looking at the first try, it seems that there's a difference. This difference can be explained by the fact that the strains developed in the tie-rod are so small, one unit change can cause a big difference in the readings. If the experiment can be performed with more tries and also plotted on a normal probability plot to show the average value of the gradient.



Graph (2) Change in length of right hand tie-rod in first two tests

Looking at the second graph, where the comparison is made with the obstacle obscuring the tie-rod movement, it can be concluded that there's a major difference in displacement - 0.0029m or 2.9mm. The tie-rod with the obstacle is receiving a much greater resistance than the other one which shows the importance of the compressive strength of materials of the component. The compressive strength limit of steel is 1GPa (CES, 2015) and the average value of compressive stress in the example is 3179.993 kPa. There is a tremendous difference between the compressive strength limit and the result in this case, although in other vehicles, such as medium sized family saloons, the results might be different and thus, the possibility of fatigue failure over time.

4.4. Third Test Readings, Results and Discussion

Third test		
Try	High-friction surface results (V)	Low-friction surface results (V)
1	0.71	0.45
2	0.35	0.45
3	0.65	0.4
4	0.35	0.46
5	0.71	0.46
6	0.36	0.46
Avg.	0.52	0.45

Table (13) Third test readings

	Force on left hand (N)	Force on right hand (N)
1	696.51	441.45
2	343.35	441.45
3	637.65	392.4
4	343.35	451.26
5	696.51	451.26
6	353.16	451.26

Table (14) Force in third test

	Stress on left hand (Pa)	Stress on right hand (Pa)
1	1980522.066	1255260.464
2	976313.6943	1255260.464
3	1813154.004	1115787.079
4	976313.6943	1283155.141
5	1980522.066	1283155.141
6	1004208.371	1283155.141

Table (15) Stress in third test

	Strain on left hand	Strain on right hand
1	0.009431057	0.005977431
2	0.004649113	0.005977431
3	0.008634067	0.005313272
4	0.004649113	0.006110263
5	0.009431057	0.006110263
6	0.004781945	0.006110263
AVG	0.006929392	0.005933154

Table (16) Strain in third test

	Displacement For left hand (m)	Displacement For right hand (m)
1	0.0028	0.0018
2	0.0014	0.0018
3	0.0026	0.0016
4	0.0014	0.0018
5	0.0028	0.0018
6	0.0014	0.0018
AVG	0.0021	0.0018

Table (17) Displacement in third test



Graph (3) Change in length in third test

Looking at the results in displacement in Graph (3), one can observe a different result, compared to the previous tests. As stated before, the steering input in this test is performed to both left and right. The Left Hand side results are taken from the tyre which is on the surface with the high-friction coefficient. Dividing the results into two

groups and looking into the data from the upper tables in the section, one can conclude that the higher values in the plot are the result from tension and the lower values are from the compression. Since this experiment is the only one that has two steering inputs, it cannot be compared to the previous results and a different approach for analysis is needed to be made:

- In an ideal world the readings for both compression and tension should be the same, since the forces and moments from the steering output don't change. If there was a difference in those forces, they would've been indicated in the opposite tie-rod as well.
- Another point that could be taken into consideration is the lack of tyre pattern. If there was a pattern on the rubber, this would've led to different behaviour of the friction coefficient, caused by the deflected thread path. If the pattern was present, a calculation and assumption could've been made by using the methods and formulas explained by Matsuda in the literature review.
- The third factor that might cause this phenomena is the changing geometry in the steering system. As the steering rack is moved, the angles between the tie-rods and the direction of travel of the wheels change. This is the most plausible explanation for the observed situation, but since the results in each tie-rod differ from each other, this factor should be excluded as well.
- The last factor that might cause those readings is a fault in the strain gauge. Since the displacement in compression on the left hand tie-rod is less than the displacement on the right hand tie-rod, one can say that the compression readings from the strain gauge are off the pattern. Another reason for this statement is the difference between the tensile and compressive strength of the material. The compressive strength has a value of 1GPa, whereas the tensile strength has a value of 2.24GPa. This confirms the above statement that the tie-rod should experience more compression than tension and thus solidifies the statement that the strain gauge gives wrong readings.

5. Conclusions

The aims and objectives of this dissertation report have been shown and met. An advanced understanding of the steering system has been developed shown in the literature review. The study on the developed strains in the tie-rods of the Formula Student vehicle has given results that could help in modern day situations. Following the discussions in the previous sections, it can be said that different conditions have effect on those developed strains:

The greatest strains, the system is experiencing are occurring when an obstacle prevents movement. Although it doesn't have an effect on the free-movement tyre, it does have a 45mm displacement on the other one and this makes it a potential reason for failure. Different failure modes can occur such as misalignment in the steering system which leads to different tyre wear around the edges. Another possible failure mode is mechanical failure in the tie-rods due to crumple, which could lead to great financial losses or even injury to the driver and the occupants. The last possible failure mode is loosening of the joints of the steering system which could also lead to an injury.

After the discussion of the third experiment it can be said that the results were inconclusive and more data needs to be gathered. A possible experiment with more trials could clarify the situation, but another way to settle the results could be to perform the test with both tyres on the same surface and both directions of steering input. This would then show if there's a difference in displacement when compressing and tensioning the tie-rods.

6. Proposal for future applications.

The data taken from this project can be used and extended in many ways. A possible continuation of the project could lead to revelations that will help designers develop better steering systems.

One possible application of the data could be to design a system that separates the steering rack into two – instead of having the steering fluid working on a single piston that moves both of the tie-rods, an alternative design with two pistons that generate movement in the tie-rods independently could be created. This design would need an

introduction of sensors that detect whether an obstacle is obscuring the wheels or if there's a difference between the surface friction coefficients under each tyre.

Bibliography

G. Demosthenous, Stratis Kanarachos, "Modeling the mechanical behavior of composite metal plastic pipes subject to internal pressure and external soil and traffic loads", Proceedings of the WSEAS international conference on Systems Science, 2007

Kanarachos, S., "Analysis of 2D flexible planar mechanisms using linear finite elements and incremental techniques", Computational Mechanics Vol 42, 2008, pp. 107-117

Spentzas, K.N, Kanarachos, S.A. "An incremental finite element analysis of mechanisms and robots", Forschung im Ingenieurwesen 67, 2002, pp. 209-219, Springer-Verlag

Stratis A. Kanarachos, Dimitris Koulocheris, "Analysis of flexible mechanisms using the conventional FEM", Proceedings of the 1st IC-SCCE (1st International conference "From Scientific Computing to Computational Engineering"), September 8 - 10, 2004, Athens, Greece.

Atanackovic, Teodor. Theory of Elasticity for Scientists and Engineers. Boston: Birkhauser, 2010

Green, A. Theoretical Elasticity. New York: Dover Publications, INC. 1992

Birch, Thomas. Automotive Suspension & Steering Systems. New York: Delmar Publishers. 1998

References

Kanarachos, Stratis. "Analysis Of 2D Flexible Mechanisms Using Linear Finite Elements And Incremental Techniques". Computational Mechanics 42.1 (2008): 107-117. Web.

Matsuda, Takuro et al. "instantaneous Estimation Of Road Friction Based On front Tire SAT Using Kalman Filter". *SAE International Journal of Passenger Cars – Mechanical Systems* 6.1 (2013): 147-153. Web.

Matilainen, Mika. "Tyre Friction Potential Estimation By Aligning Torque And Lateral Force Information". Masters of Science in Technology. AALTO University, (2011). Print.

Spentzas, K.N. and S.A. Kanarachos. "An Incremental Finite Element Analysis Of Mechanisms And Robots". *Forschung im Ingenieurwesen* 67.5 (2002): 209-219. Web.

Vishay Micro-Measurements (2005) *The Three-Wire Quarter-Bridge Circuit* [online] available from <http://www.intertechnology.com/Vishay/pdfs/TechNotes_TechTips/TT-612.pdf> [1 April 2016]

RepairPal.com (2016) *Power Steering* [online] available from <<http://repairpal.com/power-steering>> [14 April 2016]

EngineBasics (2010) *How Automotive Pump Works* [online] available from <<http://www.enginebasics.com/Engine%20Basics%20Root%20Folder/Power%20Steering.html>> [14 April 2016]

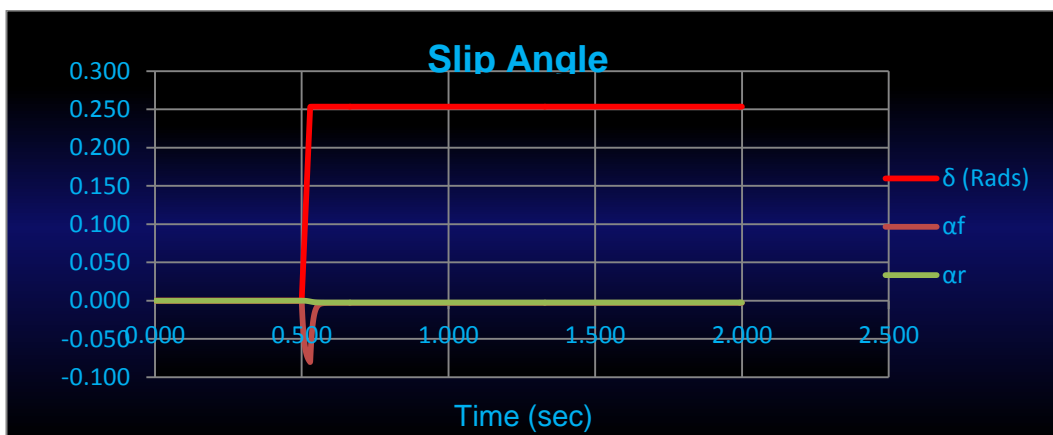
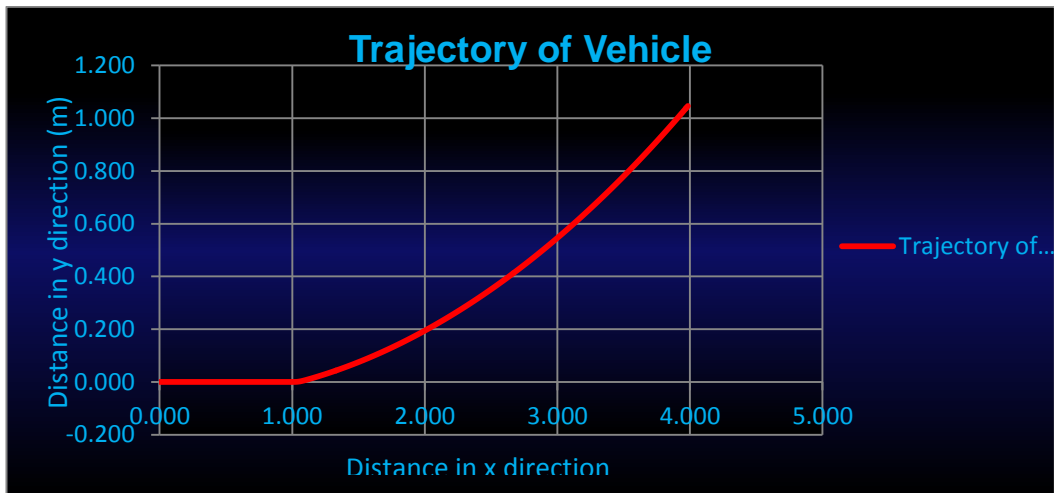
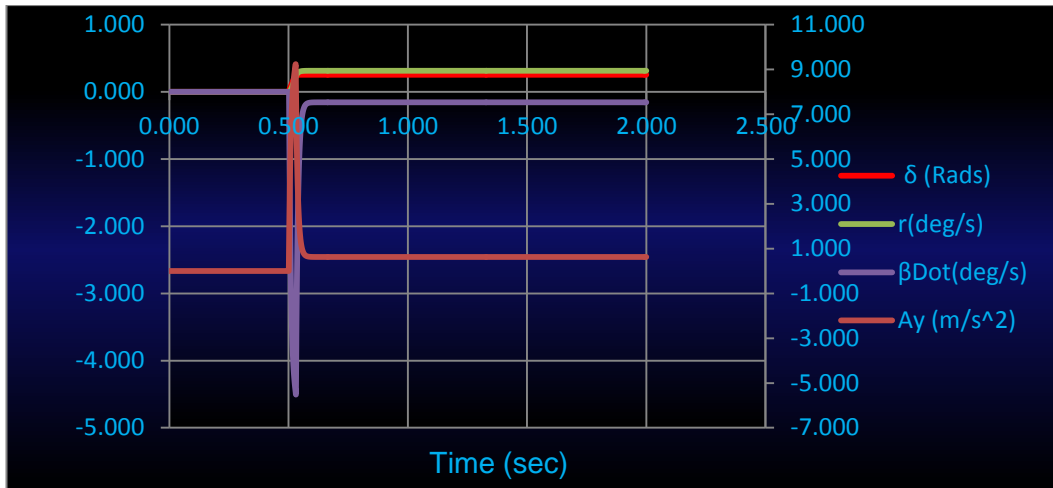
HowStuffWorks (2016) *How Car Steering Works* [online] available from <<http://auto.howstuffworks.com/steering4.htm>> [14 April 2016]

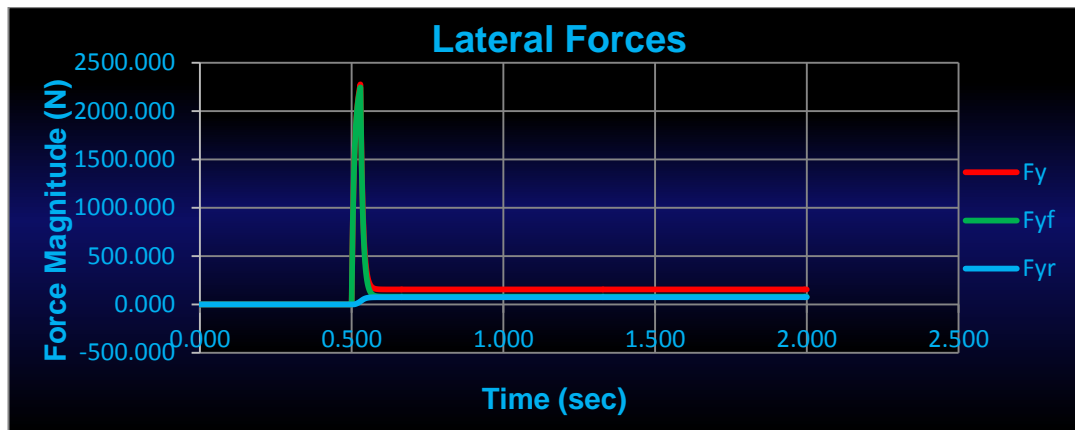
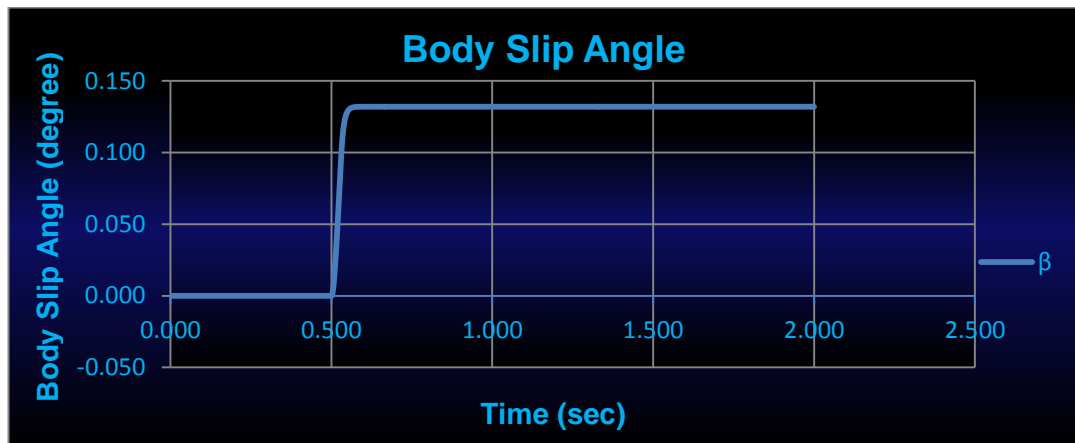
Vishay Micro-Measurements (2005) *The Three-Wire Quarter-Bridge Circuit* [online] available from <http://www.intertechnology.com/Vishay/pdfs/TechNotes_TechTips/TT-612.pdf> [15 April 2016]

Grantadesign (2016) *CES EduPack, 2015* [online] available from <<https://www.grantadesign.com/education/edupack/>> [15 April 2016]

Appendix

Bicycle model graphs:





Measurement and analysis of strains developed on tie-rods of a steering system Coventry University				S T A R T												D E A D L I N E							
Prepared By:	Stefan Aserov 2837564	Start	End	Task Description	Start	End	Duration (days)	Days Complete	Days Remaining	25/01/2016	01/02/2016	08/02/2016	15/02/2016	22/02/2016	29/02/2016	07/03/2016	14/03/2016	21/03/2016	28/03/2016	04/04/2016	11/04/2016	18/04/2016	25/04/2016
Supervisor:	Dr. Stratis Karachios	25/01/2016	12/01/2016	Aims & Objectives	25/01/2016	12/01/2016	11	1	0														
Start Date:	22/01/2016	27/01/2016	07/02/2016	Literature Review	27/01/2016	07/02/2016	11	11	0														
Date Today:	25/04/2016	05/02/2016	05/02/2016	Measurement on Car	05/02/2016	05/02/2016	1	1	0														
		08/02/2016	14/02/2016	Kinematic model	08/02/2016	14/02/2016	7	7	0														
		08/02/2016	15/02/2016	Interim Report	08/02/2016	15/02/2016	8	8	0														
		22/02/2016	13/03/2016	Design of test	22/02/2016	13/03/2016	21	21	0														
		14/03/2016	20/03/2016	Measurement of strains	14/03/2016	20/03/2016	7	7	0														
		21/03/2016	03/04/2016	Analysis	21/03/2016	03/04/2016	14	14	0														
		04/04/2016	10/04/2016	Conclusion	04/04/2016	10/04/2016	7	7	0														
		11/04/2016	17/04/2016	Future Applications proposal	11/04/2016	17/04/2016	7	7	0														
		18/04/2016	25/04/2016	Revision	18/04/2016	25/04/2016	7	7	0														
Complete		21/03/2016	25/04/2016	Development of Report	21/03/2016	25/04/2016	36	36	0														

Planned time	
Actual time	